CrossMark

TECHNICAL PAPER

Weighted principal component analysis combined with Taguchi's signal-to-noise ratio to the multiobjective optimization of dry end milling process: a comparative study

Danielle M. D. Costa[1,2] · **Gabriela Belinato**[1,2] · **Tarcísio G. Brito**[1] · **Anderson P. Paiva**[1] · **João R. Ferreira**[1,2] · **Pedro P. Balestrassi**[1]

Abstract The weighted principal component analysis (WPCA) method is a mathematical programming technique developed to optimize multiple correlated characteristics, considering the most significant principal components scores, weighted by their respective eigenvalues. This method has obtained noteworthy results, given that it reduces the data set and still considers the correlation between the responses. However, when multiple correlated characteristics also have conflicting objectives, maximizing or minimizing the WPCA can favor some variables and harm others. This paper proposes a hybrid approach able to standardize the optimization objectives of the original responses, reduce dimensions, and, at the same time, eliminate the correlation between the multiple responses.

Technical Editor: Márcio Bacci da Silva.

✉ Danielle M. D. Costa
  danielle.costa@ifsuldeminas.edu.br

  Gabriela Belinato
  gabrielabelinato@gmail.com

  Tarcísio G. Brito
  engtarc.gb@ig.com.br

  Anderson P. Paiva
  andersonppaiva@unifei.edu.br

  João R. Ferreira
  jorofe@unifei.edu.br

  Pedro P. Balestrassi
  pedro@unifei.edu.br

[1] Institute of Production Engineering and Management, Federal University of Itajubá, Bps Avenue 1303, Itajubá, Minas Gerais 37500-188, Brazil

[2] Instituto Federal do Sul de Minas – Campus Pouso Alegre, Avenida Maria da Conceição Santos 900, Parque Real, Pouso Alegre, Minas Gerais 37550-000, Brazil

This approach, called Weighted Principal Component Analysis combined with Taguchi's Signal-to-noise ratio (or WPCA-SNR), is based on Taghuchi's signal-to-noise ratio and Principal Component Analysis weighted by their respective eigenvalues. Since most of the manufacturing processes present multiple correlated characteristics and conflicting objectives, a case study based in six quality characteristics of the dry end milling process of the AISI 1045 steel is here presented to illustrate the comparative performance of two approaches, WPCA and WPCA-SNR. Theoretical and experimental results indicate that the WPCA-SNR method has evidenced acceptable solutions for both objectives, indicating feasibility of the multiobjective optimization technique applied to this process. In this case, $f_z = 0.08$ mm/tooth, $a_p = 1.62$ mm, $V_c = 331$ m/min, and $a_e = 15.49$ mm are the optimal parameters for minimizing roughness and maximizing material removal rate, simultaneously.

1 Introduction

As with most machining processes, such as end milling, the multiple quality characteristics measured are highly correlated and with different optimization objectives. The relationship between roughness and material removal rate responses can be taken as one example; while roughness has to be minimized, removal rate has to be maximized. In these cases, the task is to find a vector of decision variables that satisfies, at the same time, more than one of the

objective functions and the constraints, and provides an acceptable value for each response [1].

However, choosing parameters that provide global optimization for more than one characteristic of interest is not an easy task [2], once it requires complete understanding of process mechanism.

According to Moshat et al. [3] and Montgomery [4], when wanting to obtain the simultaneous variation of factors to build forecasting models for all relevant outputs, generally employ design of experiments (DOE), such as Taguchi arrays or Response surface methodology (RSM) or, regression techniques. However, as pointed out by many researchers [5, 6], these techniques can be greatly influenced by the correlations, causing model instability, over fitting, prediction errors, and inaccuracy on the regression coefficients. Another aspect is that the individual analysis of each response may lead to a conflicting optimum, since the factor levels that improve one response can, otherwise, degrade another [6]. In this case, the regression equations or the use of optimization methods that do not consider correlation are not adequate to represent an objective function without considering the variance–covariance structure among the multiple responses [1, 2, 5–8].

The optimization literature frequently reveals correlated responses with conflicting objectives in several end milling studies. Some of these works have been summarized in Table 1. In all these works, a strong or moderated correlation with a significant statistic among the responses was observed (this analysis was carried out by us, using the coefficient of Pearson). Although the results have been coherent, the correlation structure was not considered in these works. Just three works have assumed that correlated responses could deviate the optimization results and produce unreal solutions [1, 8, 9]. To resolve this drawback, these authors have presented a hybrid approach considering a combination of methods as PCA and RSM with multivariate mean square error (MMSE) [1], PCA and RSM [8], and PCA and grey relational analysis (GRA) [9], respectively. Moshat et al. [3] have also assumed that correlated responses could deviate the optimization results.

In addressing the correlation influence in multiobjective optimization problems, some researchers have employed the principal component analysis (PCA) as an alternative approach [1, 5–8, 10–19]. This multivariate technique summarizes, in a few uncorrelated components, common patterns of variation among response variables. While effective, this approach presents a drawback, when the first principal component score is not enough to explain most of the correlation (or variance–covariance) structure [2, 5, 6]. To overcome these shortcomings, some researchers proposed methods based on weighted principal component analysis (WPCA) [2, 20–25]. This strategy aggregates all the principal component scores weighted by their respective eigenvalues, fully explaining variations in all responses.

However, when multiple correlated characteristics also have conflicting objectives, maximizing or minimizing the weighted principal components can favor some variables and harm others. In this case, WPCA method—though capable of eliminating the correlation's effect—is unable to maximize and minimize the wanted parameters, simultaneously. Thus, the WPCA method can conduct the results to inadequate optimum solutions.

In this way, when the multiple responses present conflicting objectives and significant correlation, applying the Taguchi's Signal-to-noise ratio (SNR) before principal components analysis will solve the problem [7, 25]. In recent times, the Taguchi's signal-to-noise ratio combined with principal component analysis has been the subject of studies by many authors, such as [3, 7, 9, 11–16, 25–28]. This method has obtained noteworthy results, given that it reduces the data set, considers the correlation between the responses, avoids the production of inappropriate optimal points in the optimization problem, and considers the conflicting objectives between the multiple responses.

By analysing these works, it can be noted that only in Costa et al. [7], PCA was conducted combined with signal-to-noise ratio for RSM. In all the other publications, Taguchi design has been used to model the responses. Furthermore, only two works have combined WPCA with SNR [27, 29]. However, in both works, the Taguchi array was used. According to Paiva, Ferreira e Balestrassi [6], the main reason why PCA is more widely used with Taguchi than with response surface designs is related to the type of optimization that the multivariate objective functions must follow. The analysis in Taguchi designs is made employing the concept of loss function. Specifically, that means each kind of optimization (maximization, minimization, or normalization) can be represented by a proper signal-to-noise relation applied to the original responses. Due to the mathematical nature of this relation, the signal-to-noise ratio must always be maximized. In RSM, however, the approach is very different.

To that end, this paper proposes a hybrid multiobjective optimization approach able to standardize the optimization objectives of the original responses, reduce dimensions and, at the same time, eliminate the correlation between the multiple responses. This approach proposed is called WPCA-SNR method. A systematic procedure was developed for this very purpose. To model and optimize the problem, the WPCA-SNR combines Response Surface Methodology and Generalized Reduced Gradient (GRG) algorithm.

To demonstrate its applicability, the dry end milling process of the AISI 1045 steel was considered for a case study. Four input parameters (feed per tooth, cutting speed, axial,

Table 1 Background studies of end milling process

References	Workpiece	Cutting parameters	Responses	Solution technique	Correlation analysis[a]
Ginta et al. [31]	Titanium Alloy Ti–6Al–4V	Speed, feed, axial depth of cut	R_a and Tool life (T)	DOE (RSM), ANOVA, graphical analysis	−0.500 (p = 0.069)
Lu et al. [9]	SKD61 tool steel	Milling type, spindle speed, feed, radial and axial depth of cut	MRR, T	DOE (Taguchi), GRA, PCA	Correlation among MRR and T_i: above 0.900 (p = 0.000).
Moshat et al. [3]	Aluminum Plates	Spindle speed, feed, depth of cut	R_a and MRR	DOE (Taguchi), ANOVA, graphical analysis	0.872 (p = 0.002)
Thangarasu et al. [32]	AISI 304 Stainless Steel and Aluminum 6061	Spindle speed, feed, depth of cut, insert type	R_a and MRR	DOE (Taguchi), Box-Behnken, MOGA, ANOVA, graphical analysis	0.644 (p = 0.000)
Chahal et al. [33]	Hot H-11 Die Steel	Spindle speed, feed, depth of cut, step over, coolant pressure	R_a and MRR	One variable at a time approach (OFAT), graphical analysis	0.954 (p = 0.000) / 0.857 (p = 0.000)
Brito et al. [34]	AISI 1045 Steel	Feed per tooth, axial and radial depth of cut, cutting speed	R_a and R_t	DOE (RSM), RPD, NBI with combined arrays	0.965 (p = 0.000)
Singh et al. [35]	SAE 52100 Steel	Cutting speed, feed, depth of cut	R_a and MRR	DOE (Full Factorial) e RSM, ANOVA, graphical analysis	0.536 (p = 0.004)
Kumar and Davis [36]	AISI 410 Steel and Aluminum 6061	Spindle speed, feed, depth of cut	R_a and MRR	DOE (Taguchi), RSM, ANOVA, graphical analysis	AISI 410: −0.608 (p = 0.082) / Aluminum: −0.430 (p = 0.248)
Bhogal et al. [37]	Plate of EN-31 Steel	Cutting speed, axial feed, depth of cut	R_a, T and Cutting tool vibration (V)	DOE (Full factorial), ANOVA, graphical analysis	$R_a - T_L$ (−0.358, p = 0.067)/ $R_a - T_V$ (0.471, p = 0.013)/ $T_L - T_V$ (−0.493, p = 0.009)
Costa et al. [1]	AISI 1045 Steel	Feed per tooth, axial and radial depth of cut, cutting speed	R_a, R_y, R_q, R_z, R_t and MRR	DOE (RSM), MMSE, NBI	Correlation among Roughness: above 0.965 (p = 0.000). Correlation among Roughness and MRR: above 0.500 (p = 0.007–0.023)
Lopes et al. [8]	AISI 1045 Steel	Feed per tooth, axial and radial depth of cut, cutting speed	R_a and R_t	DOE (RSM), RPD, PCA, NBI with combined arrays	0.965 (p = 0.000)

[a] The correlation analysis was carried out by us, using the coefficient of Pearson

1666

J Braz. Soc. Mech. Sci. Eng. (2017) 39:1663–1681

and radial depth of cut) and six response variables, average surface roughness, maximum surface roughness, root-mean-square roughness, ten-point height, maximum peak to valley, and material removal rate were considered.

Although the hybrid approach between Principal Components Analysis and Taguchi's signal-to-noise ratio has already been extremely disseminated, this study differs from most approaches already proposed. First, in this study, more than two response variables, with conflicting objectives and significantly correlated, were considered in the optimization problem. Second, unlike most in the published literature studies, the mathematical models of Principal Components have been created to predict the results of different input parameters using Response Surface. Third, more than one principal component was considered. It can be noted that in the most cases, studied and published have had one eigenvalue larger than one; and thus, only the first principal component has been considered in the analyses. However, this does not occur in the majority of cases in today's complex manufacturing processes we have. Finally, it was not found another work using a weighted approach of Principal Component combined with Taguchi's signal-to-noise ratio for RSM in end milling process.

In the following sections, this paper compares the results obtained by the WPCA method and SNR-WPCA method applied on the dry end milling process.

2 Theoretical fundamentals

2.1 Weighted principal component analysis method

Principal component analysis is a multivariate analysis technique, which, in summary, is able to represent the original responses in a few number of uncorrelated latent variables, without significant loss of information [5, 6]. According to Paiva et al. [6] and Bertolini and Schiozer [28], the reduced data set consists of single or multiple components called Principal Components (PC) and are sorted from the highest variance to the lowest. Zhang et al. [30] also mentioned that, based on the variance–covariance matrix, the PCA method proceeds in such a way that the first principal component has the highest variance, and each succeeding component, in turn, has the highest possible variance within the constraint.

PCA uses the factorization of a variance–covariance Σ or correlation matrix $\mathbf{R}$ associated with the random vector $Y^T = [Y_1, Y_2, \ldots, Y_p]$, to produce pairs of eigenvalues–eigenvectors $(\lambda_i, e_i), \ldots, \geq (\lambda_p, e_p)$, where $\lambda_1 \geq \lambda_2 \geq \cdots \geq \lambda_p \geq 0$ and an uncorrelated linear combination $PC_i = e_i^T Y = e_{1i} Y_1 + e_{2i} Y_2 + \cdots + e_{pi} Y_p$, $i = 1, 2, \ldots, p$. The original data set may be then replaced by the uncorrelated linear combinations in the form of principal

components score (PC_{score}). PC_{score} can be written as $PC_{score} = [Z] \times [E]$ [2], where $\mathbf{Z}$ is the standardized data matrix and $\mathbf{E}$ is the eigenvectors matrix of the multivariate set [7]:

$$
PC_k = \mathbf{Z^T E} = \begin{bmatrix} \left(\frac{x_{11}-\bar{x}_1}{\sqrt{s_{11}}}\right) & \left(\frac{x_{21}-\bar{x}_2}{\sqrt{s_{22}}}\right) & \cdots & \left(\frac{x_{p1}-\bar{x}_p}{\sqrt{s_{pp}}}\right) \\ \left(\frac{x_{12}-\bar{x}_1}{\sqrt{s_{11}}}\right) & \left(\frac{x_{22}-\bar{x}_2}{\sqrt{s_{22}}}\right) & \cdots & \left(\frac{x_{p2}-\bar{x}_p}{\sqrt{s_{pp}}}\right) \\ \vdots & \vdots & \ddots & \vdots \\ \left(\frac{x_{1n}-\bar{x}_1}{\sqrt{s_{11}}}\right) & \left(\frac{x_{2n}-\bar{x}_2}{\sqrt{s_{22}}}\right) & \cdots & \left(\frac{x_{pn}-\bar{x}_p}{\sqrt{s_{pp}}}\right) \end{bmatrix}^T
$$

$$
\times \begin{bmatrix} e_{11} & e_{12} & \cdots & e_{1p} \\ e_{21} & e_{22} & \cdots & e_{2p} \\ \vdots & \vdots & \ddots & \vdots \\ e_{1p} & e_{2p} & \cdots & e_{pp} \end{bmatrix}. \tag{1}
$$

Many methods have been proposed to determine the number of principal components. Methods include (among others): the Kaiser's criteria, Log-Eigenvalue (LEV) diagram, Velicer's Partial Correlation Procedure, Cattell's SCREE test, cross-validation, bootstrapping techniques, cumulative percentage of total of variance, and Bartlett's test for equality of eigenvalues. Kaiser's criteria (1958) will be used in this paper, since is the most popular method [6].

According to Kaiser's criteria, only the principal components, whose eigenvalues are greater than one, and whose explained cumulative variance are greater than 80 %, can be used to replace the original responses. This criterion is adequate when it is used with the correlation matrix [6].

However, while effective, the multivariate technique PCA presents a drawback, when the optimization of only one principal component is not adequate to represent all the process data set [2, 5, 6]. In some cases, studied in the published literature, for example, the first principal component has been the only component extracted [8, 10, 11, 19]. This does not occur in the majority of cases in today's complex manufacturing processes we have [18]. In particular, it is doubtful whether the factor/level combination, determined by the first principal component only, is optimal or not [6, 8, 18].

In response to these concerns, some researchers proposed methods based on Weighted Principal Component Analysis (WPCA) [2, 20–25], based especially on Taguchi and Response Surface design.

The Eq. (2) is based on Paiva et al. [2]. approach, in which the WPCA index combines RSM and PCA and, works as following: the original responses, obtained through a central composite design (CCD-RSM), are replaced by the resulting significant principal component scores. Subsequently, considering the eigenvalues of the correlation matrix as a set of weights, a new response index can be written as such:

$$\text{WPCA} = \sum_{p=1}^{r} \left[\lambda_p(\text{PC}_p) \right] \qquad (2)$$

where, λ_p are the obtained eigenvalues of significant principal component and PC_p are the significant principal component scores that were extracted and stored from the original responses.

The ordinary least-squares (OLS) algorithm can be applying to WPCA index for obtain the second-order polynomial. With the RSM model established, the optimal point of the multiobjective problem can be found by locating the stationary point according to Eq. (3), only subjected to the constraint of the experimental region [2]. Other constraints may be added to the system according to the needs of the problem.

$$\text{Maximize WPCA} = \sum_{p=1}^{r} \left[\lambda_p(\text{PC}_p) \right]$$
$$s.t : g(x) = x^T x \leq \rho^2. \qquad (3)$$

To solve the non-linear programming problem (NLP) described in the form of Eq. (3), the GRG can be used. GRG is considered one of the most robust and most efficient methods for constrained NLP [2].

The assumption of maximization described in Eq. (3) is established supposing that the desired optimization direction for each original response is positively correlated with the multivariate index WPCA. In this respect, Paiva el al. [2] have assumed which direction of optimization of the WPCA index can be established by analysing the correlation between WPCA and each original response. If there is a positive correlation between a WPCA index and certain original response, then they will have the same optimization direction. In this case, maximizing or minimizing WPCA will imply on the maximization or minimization of each original response variable. On the other hand, if the correlation is negative, the optimization senses will be inverse. For example, if WPCA index maintains a negative correlation with certain variables (whose goal is maximization), then the maximization of the WPCA will lead to their minimization. Likewise, it could be argued that if the correlation between the two output variables is negative, the maximization of the WPCA will imply on the minimization of the other and vice versa. For this, the inspection of the eigenvectors reveals the relationship that exists between the ith WPCA index and the original responses. More details about the WPCA approach can be seen in [2]. Thus, a potential difficulty in optimizing a multivariate response as WPCA occurs due to conflicting minima and maxima in a group of variables that, for instance, must be simultaneously maximized.

When there is a positive correlation with some variables and negative correlation with other simultaneously,

multiplying the original response by a negative constant will solve the problem. This multiplication should be done before proceeding to the analysis of the principal component. However, when the responses have different optimization objectives, another likely alternative is to apply the Taguchi's signal-to-noise ratio [7], since it is considered more robust, simple, and may be efficiently applied for continuous quality improvement and quality control of process not only end milling but also any other machining operations, where multiple objectives come under consideration [3, 7].

Taguchi uses SNR to measure the quality characteristic deviating from the desired value and these characteristics vary depending on the type of problem under study, which may be classified as "smaller-the-better", "bigger-the-better", and "nominal-is-best" [38]. Their mathematical expressions are represented by the Eqs. (4), (5), and (6), respectively, where y denotes the performance indicator, subscript i is the experiment number, and N is the number of replicates of the experiment i. After the transformation, SNR must always be maximized, which makes it possible to standardize the optimization objectives for the individual responses [6].

$$\text{SNR} = -10 \log_{10} \left(\frac{\sum_{i=1}^{N} y_i^2}{N} \right) \qquad (4)$$

$$\text{SNR} = -10 \log_{10} \left(\frac{\sum_{i=1}^{N} 1/y_i^2}{N} \right) \qquad (5)$$

$$\text{SNR} = 10 \log_{10} \left[\left(\frac{\bar{y}}{s} \right)^2 \right], \bar{y} = \frac{y_1 + y_2 +, \cdots, + y_N}{N},$$
$$\text{and } s = \frac{\sum_{i=1}^{N} (y_i - \bar{y})^2}{N-1}. \qquad (6)$$

2.2 The weighted principal component analysis and signal-to-noise ratio applied to the multiobjective optimization

Given the discussion above, this paper proposes a hybrid approach able to standardize the optimization objectives of the original responses, to reduce dimensions, and, at the same time, to eliminate the correlation between the multiple responses. This approach, called WPCA-SNR method, is based on Taguchi's signal-to-noise ratio and Principal Component Analysis weighted by their respective eigenvalues.

The SNR-WPCA proposes that before constñructing the objective function and before carrying out the Principal Component Analysis, the signal-to-noise ratio must be applied to the original responses. A four-step process was developed to better understand the proposal approach, as it follows:

Step A: Apply the Taguchi's signal-to-noise ratio for roughness responses according to Eq. (4) and for MRR according to Eq. (5). Then, establish the Response Surface models on the normalized responses.

Step B: Perform the Principal Component Analysis on the normalized responses by Taguchi's signal-to-noise ratio using the correlation matrix. Store their respective scores, eigenvalues, and eigenvectors. Then, using the scores obtained, establish Response Surface models for the significant principal components.

Step C: Based on Eq. (2), develop the SNR-WPCA index. In this work, SNR-WPCA was developed as such Eq. (7), where, $SNRPC_p$ are the principal component scores that were extracted from the signal-to-noise ratio responses. Then, establish the Response Surface models on SNR-WPCA index. This model is the new response of the optimization problem.

$$\text{SNR-WPCA} = \sum_{p=1}^{r} \left[\lambda_p (\text{SNRPC}_p) \right]. \tag{7}$$

Step D: Based on Eq. (3), promote the optimization of the dry end milling process according to Eq. (8). In WPCA-SNR approach, the optimal points were identified using the GRG algorithm, available from Microsoft Excel's Solver®, on the respective presented formulation. The set of constraints $g(x) = x^T x \leq \rho^2$ represents the experimental region, but other constraints can be added if it is necessary.

$$\text{Maximize SNR-WPCA} = \sum_{p=1}^{r} \left[\lambda_p (\text{SNRPC}_p) \right]$$

$$\text{s.t} : g(x) = x^T x \leq \rho^2. \tag{8}$$

In terms of design factors, this proposal establishes the empirical models for multiple responses of the dry end milling process, but can be applied to any manufacturing process.

3 Experimental method

The multiobjective optimization of dry end milling process employing to WPCA-SNR approach can be described at three stages. In the first stage, the Response Surface Methodology (RSM) was employed to determine the objective functions for the original responses. RSM combines statistical experimental design principles and mathematical techniques which are useful for the modelling and analysis of problems, in which responses of interest are not known and are influenced by several variables [4]. In the second stage, the correlation structure among the responses was analysed and the process was optimized by the WPCA method, thereby obtaining a primary optimal solution; it characterized the necessity of standardization the original response.

Therefore, Taguchi's signal-to-noise ratio was applied for the original responses, and then, the third stage was initiated. In the third stage, the proposal SNR-WPCA approach was applied, identifying a new optimal solution based on Taguchi's signal-to-noise ratio and Principal Component Analysis weighted by their respective eigenvalues. At the end, the results obtained by the WPCA method and SNR-WPCA method applied on the dry end milling process were compared.

## 3.1 Experimental procedure and data analysis

In this work, the end milling parameters defined as input variables were feed per tooth (f_z), axial depth of cut (a_p), Cutting speed (V_c), and radial depth of cut (a_e). These parameters were designed according to a central composite design (CCD), created for four parameters at two levels totalling 16 factorials $\left(2^k = 2^4 = 16 \right)$, eight axial points ($2k = 8$), and six center points. The additional centre point can be used to check for curvature. Furthermore, multiplying the centre points is strongly recommended, since they can improve the estimates of the quadratic effects and allow additional degrees of freedom for error. In coded units, the centre points present values 0 [4] (Table 4). To specify the parameter levels, previous studies and preliminary tests were considered. The parameter levels were fixed, as shown in Table 2. In the CCD matrix, a coded distance (ρ) of 2.0 was adopted for the centre points to the axial points. The experiments were conducted in a random order, but the data were arranged in standard order for easier viewing of the experimental designing. The software Minitab® was used to build the experimental matrix and to perform the statistical analysis from the experimental data.

The set of the outputs variables included average surface roughness (R_a), maximum surface roughness (R_y), root-mean-square roughness (R_q), ten-point height (R_z), maximum peak to valley (R_t), and material removal rate (MRR). We selected five roughness's responses, because although they are considered similar in evaluating the machined surface roughness, these parameters have not the same individual optimal points. Furthermore, they are highly correlated objective functions and have conflicting objectives with the MRR. Overall, since roughness and MRR exhibit positive

Table 2 Cutting parameters and respective levels

Cutting parameters	Levels (uncoded and coded)				
	−2	−1	0	+1	+2
Feed per tooth (f_z, mm/tooth)	0.05	0.10	0.15	0.20	0.25
Axial depth of cut (a_p, mm)	0.375	0.750	1.125	1.500	1.875
Cutting speed (V_c, m/min)	275	300	325	350	375
Radial depth of cut (a_e, mm)	13.5	15.0	16.5	18.0	19.5

Fig. 1 **a** End milling tool, **b** cutting inserts, **c** workpiece
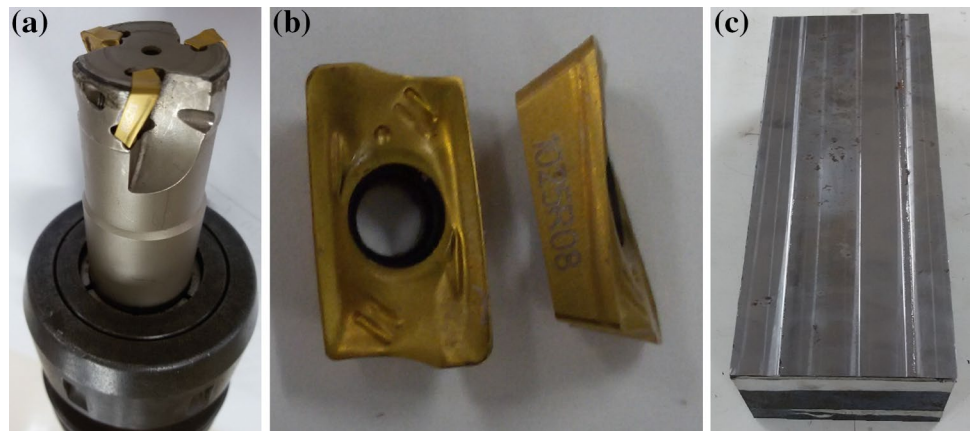
correlation and considering that these objective functions are conflicting, there is a trade-off, where the WPCA-SNR approach could satisfactorily solve the problem.

MRR (cm³/min) in end milling process was calculated as follows:

$$\text{MRR}_i = \frac{V_{f_i} \times a_{p_i} \times a_{e_i}}{1000} = \frac{f_z \times N \times Z \times a_p \times a_e}{1000} \quad (9)$$

with V_f (table feed, mm/min), N (spindle speed, RPM), Z (number of effective teeth of the tool, $Z = 3$), and i (number of experiments). N can be calculated as $N_i = \frac{V_{c_i} \times 1000}{\pi \times \text{DC}_{ap}}$, where DC_{ap} (cutting diameter at cutting depth, of the tool, $\text{DC}_{ap} = 25$ mm).

The experiments were conducted on an FADAL, vertical machining center, model VMC 15, Maximum power of 15 kW, and maximum rotation speed of 7500 RPM. The tool overhang was 60 mm. The tool used was a positive end mill, code R390-025A25-11M with a 25 mm diameter, entering angle of $\chi_r - 90°$, and a medium step with three inserts (Fig. 1a). Three rectangular inserts were used with edge lengths of 11 mm each, code R390-11T308M-PM GC 1025 (Fig. 1b). The insert material used was cemented carbide ISO P10 coated with TiCN and TiN by the PVD process. The coating hardness was around 3000 HV3 and the substrate hardness 1650 HV3 with a grain size smaller than one. The surface roughness of the machined workpiece was measured using a Mitutoyo portable roughness meter, model Surftest SJ 201, with a cut-off length of 0.25 mm. All the milling experiments were performed under dry conditions.

The workpiece material was AISI 1045 steel (Fig. 1c), with hardness of approximately 180 HB. The dimensions of the workpiece were rectangular blocks square sections of 100 × 100 mm and lengths of 300 mm. In the present days, AISI 1045 is widely used for all industrial applications requiring more wear resistance and strength. This material shows good machinability in normalized as well as the hot rolled condition. Based on the recommendations

Table 3 Chemical composition of AISI 1045 steel

Element	Fe	C	Mn	P_{max}	S_{max}
(%)	98.510–98.980	0.420–0.500	0.600–0.900	0.040	0.050

given by the machine manufacturers, operations, such as tapping, milling, broaching, drilling, turning, and sawing, etc, can be carried out on AISI 1045 steel using suitable feeds, tool type, and speeds. The chemical composition of this steel is given in Table 3.

Once all the responses had been measured, they were assembled to compose the experimental matrix presented in Table 4 and used as a data source for the modelling and optimization of the process.

Experimentally, two least-squares-based models can be obtained: coded and uncoded based parameters. Montgomery [4] considers that the statistical analyses of the results are usually carried out using the coded variables. However, the same author says that it is often necessary to convert coded units into the original responses. For quantitative variables, uncoded variables can be achieved by the inverse of the following:

$$X_i = \frac{x_i - \bar{x}_i}{\frac{1}{2}\Delta x_i} \quad (10)$$

where X_i stands for the coded value of the ith variable, x_1 stands for the original value of the ith variable, $\bar{x}_1$ stands for the center point value of the original ith variable, and Δx_i stands for the difference of the original two values of the ith variable. The half value of the difference is called the step size [4].

The coded units approach is better than uncoded, because it provides resources to eliminate any spurious statistical results due to different measurement scales for the factors. In addition, uncoded units often lead to collinearity among the terms in the model. This inflates the variability

Table 4 Experimental design–central composite design matrix

Exp. No	Cutting parameters								Original responses					
	Coded units				Uncoded units				Min.					Max.
	f_z	a_p	V_c	a_e	f_z	a_p	V_c	a_e	R_a	R_y	R_z	R_q	R_t	MRR
1	−1	−1	−1	−1	0.10	0.75	300	15.00	1.18	5.53	5.16	1.37	5.63	12.89
2	1	−1	−1	−1	0.20	0.75	300	15.00	1.98	9.71	8.86	2.34	10.04	25.78
3	−1	1	−1	−1	0.10	1.50	300	15.00	1.17	5.01	4.76	1.36	5.14	25.78
4	1	1	−1	−1	0.20	1.50	300	15.00	1.48	7.89	7.00	1.82	7.94	51.57
5	−1	−1	1	−1	0.10	0.75	350	15.00	1.15	4.75	4.44	1.31	4.76	15.04
6	1	−1	1	−1	0.20	0.75	350	15.00	2.08	9.27	8.74	2.43	9.48	30.08
7	−1	1	1	−1	0.10	1.50	350	15.00	1.10	5.06	4.62	1.25	5.16	30.08
8	1	1	1	−1	0.20	1.50	350	15.00	1.69	8.05	7.39	2.00	8.30	60.16
9	−1	−1	−1	1	0.10	0.75	300	18.00	1.04	5.78	4.78	1.21	5.85	15.47
10	1	−1	−1	1	0.20	0.75	300	18.00	1.67	8.03	7.65	2.06	8.17	30.94
11	−1	1	−1	1	0.10	1.50	300	18.00	1.16	5.22	4.95	1.34	5.38	30.94
12	1	1	−1	1	0.20	1.50	300	18.00	1.82	9.13	8.18	2.19	9.27	61.88
13	−1	−1	1	1	0.10	0.75	350	18.00	1.19	5.33	5.13	1.37	5.49	18.05
14	1	−1	1	1	0.20	0.75	350	18.00	1.99	8.86	8.32	2.35	8.88	36.10
15	−1	1	1	1	0.10	1.50	350	18.00	1.18	5.13	4.79	1.36	5.35	36.10
16	1	1	1	1	0.20	1.50	350	18.00	1.74	8.52	7.48	2.07	8.74	72.19
17	−2	0	0	0	0.05	1.12	325	16.50	0.37	2.68	2.00	0.45	2.73	11.52
18	2	0	0	0	0.25	1.12	325	16.50	1.86	9.12	8.71	2.26	9.28	57.61
19	0	−2	0	0	0.15	0.37	325	16.50	1.54	6.69	5.99	1.75	6.84	11.52
20	0	2	0	0	0.15	1.87	325	16.50	1.16	6.13	5.47	1.39	6.20	57.61
21	0	0	−2	0	0.15	1.12	275	16.50	1.55	7.18	6.54	1.80	7.34	29.25
22	0	0	2	0	0.15	1.12	375	16.50	1.61	7.25	6.83	1.87	7.52	39.88
23	0	0	0	−2	0.15	1.12	325	13.50	1.56	6.87	6.52	1.81	7.07	28.28
24	0	0	0	2	0.15	1.12	325	19.50	1.60	7.09	6.72	1.85	7.49	40.85
25	0	0	0	0	0.15	1.12	325	16.50	1.57	6.90	6.48	1.82	7.10	34.57
26	0	0	0	0	0.15	1.12	325	16.50	1.63	7.22	6.81	1.90	7.39	34.57
27	0	0	0	0	0.15	1.12	325	16.50	1.66	7.35	6.90	1.94	7.43	34.57
28	0	0	0	0	0.15	1.12	325	16.50	1.59	7.25	6.59	1.83	7.39	34.57
29	0	0	0	0	0.15	1.12	325	16.50	1.61	7.18	6.70	1.87	7.33	34.57
30	0	0	0	0	0.15	1.12	325	16.50	1.61	7.18	6.69	1.85	7.32	34.57

in the coefficients estimates and makes them difficult to interpret. For these reasons, it was employed the model based on the coded units [4, 6].

4 Results and discussion

4.1 Development of mathematical model

Considering the goal to analyse the relation among end milling input parameters and responses, response surface models for the six end milling characteristics were developed. According to RSM, a lower order polynomial is usually employed. However, if the experimental space is in a region of curvature, then the process is fine-tuned by a second-order polynomial, such as described by the following [4]:

$$\hat{y}(x) = \beta_0 + \beta_1 f_z + \beta_2 a_p + \beta_3 V_c + \beta_4 a_e + \beta_{11} f_z^2$$
$$+ \beta_{22} a_p^2 + \beta_{33} V_c^2 + \beta_{44} a_e^2 + \beta_{12} f_z a_p + \beta_{13} f_z V_c$$
$$+ \beta_{14} f_z a_e + \beta_{23} a_p V_c + \beta_{24} a_p a_e + \beta_{34} V_c a_e + \varepsilon$$

$$(11)$$

where $\hat{y}(x)$ represents the responses variables R_a, R_y, R_q, R_z, R_t, and MRR, f_z, a_p, V_c, and a_e are the cutting parameters, β_{ij} are coefficients to be estimated, and ε is the error observed in the response.

The values of the coefficients of the polynomials were estimated by Ordinary Least-Squares (OLS) algorithm.

Table 5 Estimated coefficients for the final quadratic models and ANOVA results

Coefficient	R_a	R_y	R_z	R_q	R_t	MRR
Constant	**1.61**	**7.18**	**6.69**	**1.87**	**7.33**	**34.57**
f_z	**0.34**	**1.69**	**1.60**	**0.43**	**1.72**	**11.52**
a_p	**−0.07**	**−0.18**	**−0.21**	**−0.07**	**−0.18**	**11.52**
V_c	0.03	−0.05	0.01	0.02	−0.04	**2.66**
a_e	0.00	0.05	0.03	0.01	0.06	**3.14**
f_z^2	**−0.11**	**−0.27**	**−0.29**	**−0.11**	**−0.28**	0.00
a_p^2	**−0.05**	−0.14	**−0.19**	**−0.06**	−0.15	0.00
V_c^2	0.00	0.06	0.05	0.01	0.07	0.00
a_e^2	0.00	0.00	0.03	0.01	0.04	0.00
$f_z \times a_p$	**−0.07**	**−0.08**	**−0.20**	**−0.07**	−0.10	**3.84**
$f_z \times V_c$	0.03	0.08	0.06	0.03	0.08	**0.89**
$f_z \times a_e$	0.00	−0.09	−0.06	0.01	−0.13	**1.05**
$a_p \times V_c$	−0.03	0.02	−0.05	−0.03	0.06	**0.89**
$a_p \times a_e$	**0.06**	0.20	**0.18**	**0.06**	0.23	**1.05**
$V_c \times a_e$	0.01	0.04	0.05	0.02	0.05	**0.24**
Adj.R^2 (%)	93.84	92.78	94.32	95.11	92.94	99.90
Standard error (S)	0.09	0.43	0.37	0.09	0.44	0.48
Regression p value	0.00	0.00	0.00	0.00	0.00	0.00
VIF	<1.10	<1.10	<1.10	<1.10	<1.10	<1.10
Normality (AD) test	0.31	0.51	0.33	0.26	0.55	2.53
Normality (AD) p value	0.54	0.12	0.51	0.68	0.14	<5 %
Curvature p value	0.00	0.00	0.00	0.00	0.00	*

Bold values represent the individually significant terms (p value <5 %)

Then, the ANOVA procedure was applied to check the adequacies of the models as well as their adjustments and to remove non-significant terms. Table 5 presents the obtained coefficients for the final full quadratic models and the main results of the ANOVA.

Regarding the adequacy, all regressions presented lower error S values. Furthermore, all regression p value presented less than 5 % significance. These results indicate that all expressions are adequate. Another important aspect in the statistical model-building process is associated with the amount of explicability of the dependent variables (y) by the predictors (x). It can be noted that the models found in the present work are adequate, once all of them exhibit Adj.R^2 above 85 % [17]. The results of the normality test for the residuals of the RSM models showed that the residuals are normal, since all Anderson–Darling coefficients (AD) were less than 1.000 (with p values higher than 5 % of significance). The Variance Inflation Factor (VIF) was also assessed. VIF values close to one imply that the predictors are not correlated. On the other hand, VIF values greater than five suggest that the regression coefficients were poorly estimated. All models showed VIF values close to one, indicating that the predictors were not correlated and were well estimated.

Table 5 also shows the calculated curvature p values for the responses. It indicates that the experimental space for

the roughness responses falls within the curvature region (p values less than 5 % of significance). As MRR is not an experimental response, there is no guarantee that the MRR equation will present curvature.

Although some non-significant terms were found, their exclusion from the complete model did not imply in prediction variance reduction of the error S and reduced Adj.R^2.

Therefore, the ANOVA results have showed that the developed models are reliable and can be used in predicting, controlling, and optimizing this dry end milling process of the AISI 1045 steel.

The analysis of variance for Response surface models and the main effects of process parameters on mean response characteristic are presented in Fig. 2. The results have shown that feed per tooth is the most influential factor to explain the behaviour of roughness responses, followed by axial depth of cut, whereas cutting speed and radial depth of cut have no impact on the roughness. On the other hand, MRR has been strongly influenced by feed per tooth and axial depth of cut, while cutting speed and radial depth of cut have a slight impact on MRR. These same results can also be found in Brito et al. [34], Charnjeet et al. [35], Costa et al. [1, 7], and Lopes et al. [8].

In fact, the authors described in Table 1 for end milling process have also published similar results. In Ginta et al. [31], for example, R_a is also more affected by the feed,

(a) Main effect for R_a

(b) Main effect for R_y

(c) Main effect for R_z

(d) Main effect for R_q

(e) Main effect for R_t
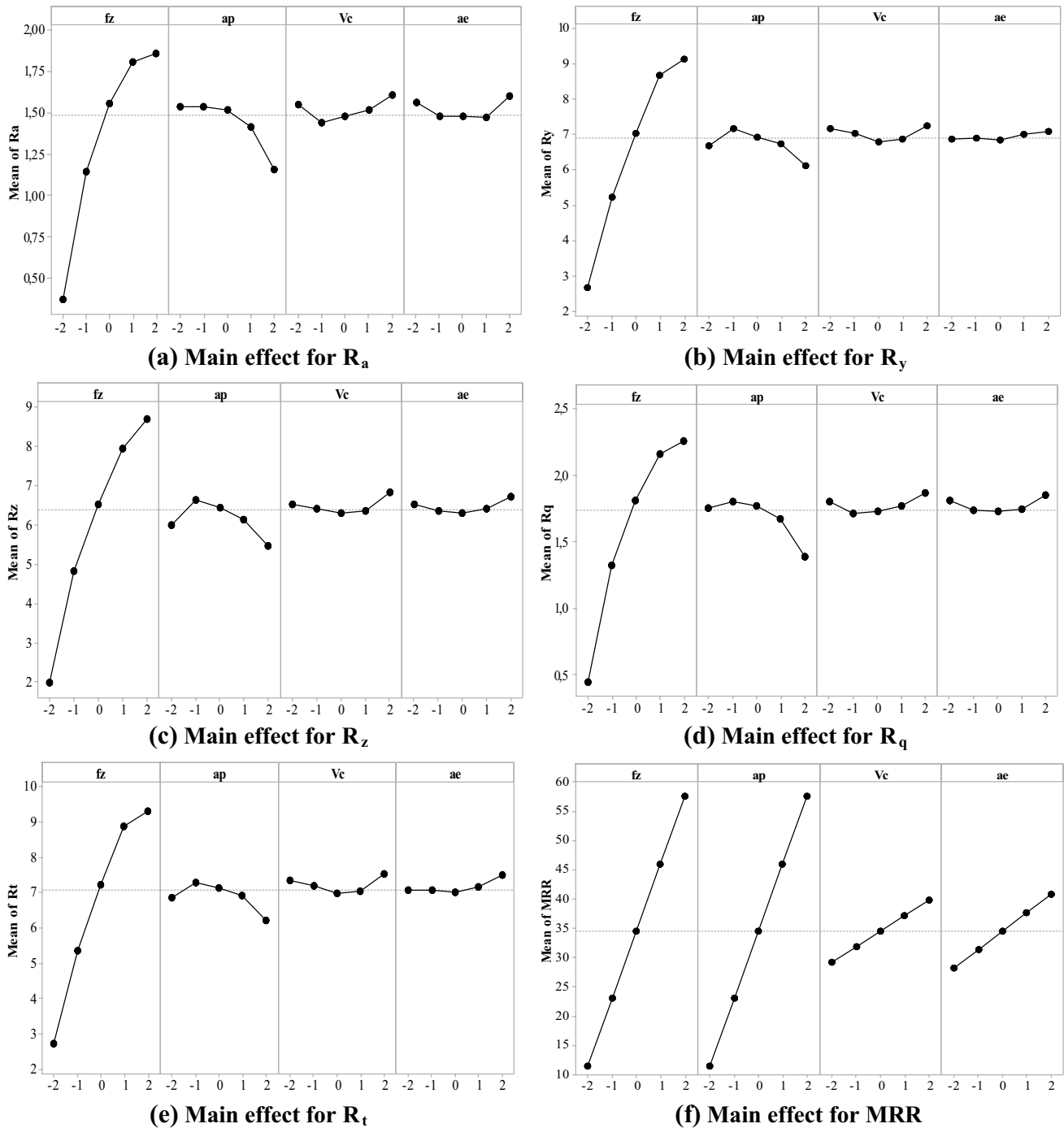

(f) Main effect for MRR

Fig. 2 Effects of process parameters on mean response characteristic

followed by cutting speed and axial depth of cut. According to authors, this is related to the effect of vibration, built-up edge, and other phenomena that occur during machining. Thangarasu, Devaraj, and Sivasubramanian [32], on the other hand, have affirmed that R_a is more affected by the depth of cut and feed rate than that of the spindle speed, so that the depth of cut is the most critical factor for attaining the MRR while reducing the value of R_a. At the same time,

in Chahal et al. [33], R_a has been significantly influenced by table feed rate and step over followed by spindle speed and depth of cut. Coolant pressure has a slight impact on surface roughness. On the other hand, MRR has been significantly influenced by depth of cut and step over followed by feed rate and spindle speed, whereas coolant pressure has no impact on MRR. Finally, in Kumar e Davis [36], the only significant factor found for the end milling operation

Table 6 Correlation structure between the responses

	R_a	R_y	R_z	R_q	R_t
R_y	0.956 (0.000)				
R_z	0.976 (0.000)	0.990 (0.000)			
R_q	0.996 (0.000)	0.972 (0.000)	0.990 (0.000)		
R_t	0.955 (0.000)	0.999 (0.000)	0.990 (0.000)	0.969 (0.000)	
MRR	0.481 (0.023)	0.557 (0.007)	0.512 (0.015)	0.508 (0.016)	0.561 (0.007)

Cells: Pearson correlation (*P* value)

Table 7 Principal component analysis: WPCA method

Eigenvalue (λ_{ij})	5.254	0.683	0.058	0.007	0.002	0.000
Proportion	0.875	0.114	0.010	0.001	0.000	0.000
Cumulative	0.875	0.989	0.999	1.000	1.000	1.000
Eigenvectors (e_{ij})	PC_1	PC_2	PC_3	PC_4	PC_5	PC_6
R_a	0.425	−0.212	0.601	−0.391	−0.298	0.415
R_y	0.433	−0.057	−0.493	−0.238	0.571	0.428
R_z	0.434	−0.105	−0.106	0.815	−0.266	0.233
R_q	0.430	−0.165	0.392	0.137	0.504	−0.601
R_t	0.433	−0.056	−0.462	−0.327	−0.510	−0.478
MRR	0.268	0.954	0.133	−0.007	−0.004	0.011

of AISI Steel 410 was speed, whose effect on the surface roughness has to be considered. While none of the factors were found to be significant for the milling operation of Aluminum 6061.

Therefore, the results above-mentioned prove that feed per tooth, axial depth of cut, and cutting speed appear to have been the most important factors on the roughness and the MRR in the end milling process.

4.2 Correlation analysis

Using correlation analysis, the existence of a strong, positive correlation, with statistical significance, between the roughness responses, and a moderate, positive correlation between roughness responses and MRR can be observed (Table 6).

Since the responses of the dry end milling process are multi-correlated, using PCA method to optimize is thus justified. In the following sections, these components are optimized using the weighted approach of Principal Component, and weighted Principal Component with Taguchi's signal-to-noise ratio approach, to decide optimal factor levels.

4.3 Optimization by the weighted principal component analysis method (WPCA)

The Principal Component Analysis was first performed to find the uncorrelated principal components needed to represent the original responses. Thus, using the correlation matrix, the principal components scores were extracted from the original responses and stored (Table 8) with their respective eigenvalues and eigenvectors (Table 7). The first and second principal components are responsible for of 99 % of the variation structure of the six dry end milling responses (Table 7).

By Kaiser's criteria, only PC_1 could be use in the optimization. However, it can be noted that, while PC_1 represents the roughness responses, since the coefficients of these terms have the same signal and are not close to zero, PC_2 represents the MRR response. In other words, there is a strong positive correlation between PC_1 and the quality characteristics studied, and a strong positive correlation between PC_2 and MRR. Thus, it is necessary to select both PC's. Thus, most of the data structure can be captured in two underlying dimensions. The remaining principal components account for a very small proportion of the variability and are considered unimportant.

To performing PC_1 and PC_2 as a valid method, it is important to check for outliers, because they can significantly influence your results. The observations' squared Mahalanobis distance can be used for this type of situation. The squared Mahalanobis distances accounts for the distance between and a group and an observation to identify outliers in the multivariate space. A point above the line reference represents an unusual observation [39]. According to Groot, Postma, and Melssen [39], it is a more powerful multivariate method for detecting outliers
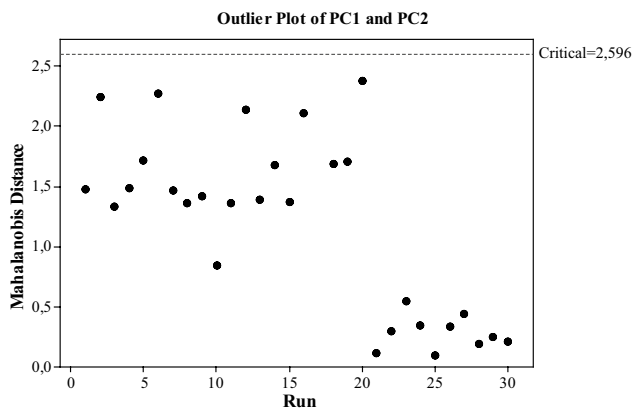
1674

J Braz. Soc. Mech. Sci. Eng. (2017) 39:1663–1681

Fig. 3 Multivariate outlier's detection for WPCA method

than examining one variable at a time, because it considers the different scales between variables and the correlations among them.

Thus, an outlier identification plot was included to assess eventual observations that could influence the inflation of regression coefficients (Fig. 3). All points are located below the reference line. This implies that the multivariate approach is an adequate option for the end milling data and that only the first two principal components are necessary to form the WPCA index.

Considering the scores calculated in the PCA (Table 8) and modelling them according to RSM, Eqs. (12) and (13) were obtained. To OLS algorithm was employed to estimate the coefficients.

Table 8 Results for WPCA method and SNR-WPCA method

	WPCA method			Signal-to-noise responses						SNR-WPCA method		
	PC_1	PC_2	WPCA	SNR/R_a	SNR/R_y	SNR/R_z	SNR/R_q	SNR/R_t	SNR/MRR	$SNR-PC_1$	$SNR-PC_2$	SNR-WPCA
1	−2.19	−0.82	−12.08	−1.44	−14.85	−14.25	−2.73	−15.01	22.21	3,08	−1,33	14,93
2	3.27	−1.43	16.18	−5.93	−19.74	−18.95	−7.38	−20.03	28.23	−3,17	−1,30	−17,40
3	−2.37	0.04	−12.44	−1.36	−14.00	−13.55	−2.67	−14.22	28.23	3,31	0,22	17,31
4	1.03	0.90	6.03	−3.41	−17.94	−16.90	−5.20	−18.00	34.25	−0,91	0,88	−4,04
5	−2.89	−0.54	−15.55	−1.21	−13.53	−12.95	−2.35	−13.55	23.55	4,14	−0,82	20,81
6	3.25	−1.22	16.24	−6.36	−19.34	−18.83	−7.71	−19.54	29.57	−3,20	−1,04	−17,36
7	−2.52	0.39	−12.94	−0.83	−14.08	−13.29	−1.94	−14.25	29.57	3,58	0,70	19,07
8	1.86	1.19	10.56	−4.56	−18.12	−17.37	−6.02	−18.38	35.59	−1,75	0,95	−8,34
9	−2.46	−0.51	−13.26	*	*	*	*	*	23.79	*	*	*
10	1.43	−0.62	7.06	4.45	18.90	17.67	6.28	18.24	29.81	−1,46	−0,49	−7,93
11	−2.15	0.34	−11.03	−1.29	−14.35	−13.89	−2.54	−14.62	29.81	3,00	0,60	15,99
12	3.00	1.02	16.43	−5.20	−19.21	−18.26	−6.81	−19.34	35.83	−2,84	0,77	−14,12
13	−2.19	−0.50	−11.85	−1.51	−14.53	−14.20	−2.73	−14.79	25.13	3,02	−0,61	15,17
14	2.78	−0.70	14.13	−5.98	−18.95	−18.40	−7.42	−18.97	31.15	−2,79	−0,53	−14,85
15	−2.09	0.65	−10.53	−1.44	−14.20	−13.61	−2.67	−14.57	31.15	2,96	0,92	16,03
16	2.46	1.83	14.16	−4.81	−18.61	−17.48	−6.32	−18.83	37.17	−2,24	1,25	−10,65
17	−6.52	0.35	−33.98	*	*	*	*	*	21.23	*	*	*
18	3.19	0.67	17.21	−5.39	−19.20	−18.80	−7.08	−19.35	35.21	−3,05	0,54	−15,38
19	−0.55	−1.40	−3.83	−3.75	−16.51	−15.55	−4.86	−16.70	21.23	0,88	−2,21	2,87
20	−1.03	1.85	−4.16	−1.29	−15.75	−14.76	−2.86	−15.85	35.21	1,74	1,80	10,38
21	0.24	−0.42	0.96	−3.81	−17.12	−16.31	−5.11	−17.31	29.32	−0,18	−0,31	−1,17
22	0.71	0.14	3.81	−4.14	−17.21	−16.69	−5.44	−17.52	32.02	−0,68	0,25	−3,33
23	0.08	−0.46	0.11	−3.86	−16.74	−16.28	−5.15	−16.99	29.03	−0,01	−0,38	−0,34
24	0.61	0.23	3.36	−4.08	−17.01	−16.55	−5.34	−17.49	32.22	−0,56	0,33	−2,65
25	0.22	−0.09	1.08	−3.92	−16.78	−16.23	−5.20	−17.03	30.77	−0,15	0,04	−0,75
26	0.62	−0.20	3.13	−4.24	−17.17	−16.66	−5.58	−17.37	30.77	−0,61	−0,07	−3,21
27	0.77	−0.24	3.87	−4.40	−17.33	−16.78	−5.76	−17.42	30.77	−0,77	−0,12	−4,08
28	0.45	−0.13	2.28	−4.03	−17.21	−16.38	−5.25	−17.37	30.77	−0,41	0,00	−2,12
29	0.52	−0.17	2.60	−4.15	−17.12	−16.52	−5.45	−17.30	30.77	−0,49	−0,04	−2,57
30	0.49	−0.16	2.44	−4.14	−17.12	−16.51	−5.34	−17.29	30.77	−0,46	−0,03	−2,40

* Denotes an observation with a large standardized residual

$$PC_1 = 0.510 + 2.390f_z - 0.114a_p + 0.086V_c + 0.100a_e$$
$$- 0.473f_z^2 - 0.255a_p^2 + 0.061V_c^2 + 0.029a_e^2$$
$$- 0.187f_za_p + 0.134f_zV_c - 0.052f_za_e - 0.044a_pV_c$$
$$+ 0.319a_pa_e + 0.073V_ca_e$$
$$\text{Adj} - R^2 = 95.26\%$$
(12)

$$PC_2 = -0.165 + 0.106f_z + 0.801a_p + 0.137V_c + 0.183a_e$$
$$+ 0.149f_z^2 + 0.078a_p^2 - 0.013V_c^2 - 0.008a_e^2$$
$$+ 0.321f_za_p + 0.017f_zV_c + 0.073f_za_e$$
$$+ 0.084a_pV_c - 0.023a_pa_e - 0.005V_ca_e$$
$$\text{Adj} - R^2 = 97.38\%.$$
(13)

The WPCA values reported in Table 8, obtained according to Eq. (2), turn into $WPCA = \lambda_1(PC_1) + \lambda_2(PC_2)$, and has considered the first eigenvalue as ($\lambda_1 = 5.254$) and second eigenvalue as ($\lambda_2 = 0.683$), according to Table 7. Applying the OLS algorithm, the multivariate objective function can be written as:

$$WPCA = 2.567 + 12.619f_z - 0.0054a_p + 0.544V_c + 0.650a_e$$
$$- 2.382f_z^2 - 1.2285a_p^2 + 0.310V_c^2 + +0.149a_e^2$$
$$- 0.763f_za_p + 0.716f_zV_c - 0.223f_za_e$$
$$- 0.175a_pV_c + 1.657a_pa_e + 0.381V_ca_e$$
$$\text{Adj} - R^2 = 95.58\%.$$
(14)

The ANOVA results for PC_1, PC_2, and WPCA expressions presented lower error S values, and the regression p value represented less than 5 % of significance. The models presented Adj.R^2 value above 85 %. These results indicate that all expressions are adequate and the full quadratic models of PC_1, PC_2, and WPCA were considered. Figure 4 represents the WPCA multivariate objective function as a function of the variables f_z and a_p, given that feed per tooth (f_z) and axial depth of cut (a_p) were the most significant for all expressions.

As previously mentioned, the direction of optimization of the WPCA index can be established by analysing the correlation between WPCA and each original response. The inspection of the eigenvectors reveals the kind of relationship that exists between the ith WPCA index and the original responses.

Examining the eigenvectors (Table 7), it is possible to observe that although there is a reasonable explanation observed between PC1 and MRR response, roughness is mainly composed by the first principal component. On the other hand, MRR is mostly composed by PC2. Furthermore, the direction of optimization (or direction of correlation) between PC_1 and all the responses is positive. On the other hand, the direction of optimization (or direction of correlation) between roughness and PC_2 is negative, while the direction of optimization is positive for PC_2 and MRR.
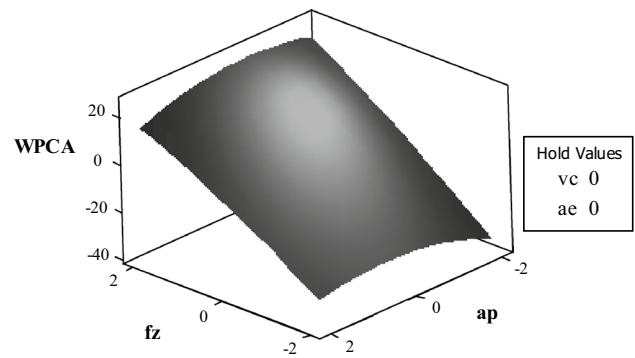

Fig. 4 WPCA surface plot as a function of a_p and f_z

Primarily, when PC_1 is maximized, all the responses will also be maximized, and minimizing PC_1 implies in minimizing all responses. When PC_2 is maximized, roughness will be minimized and MRR values will be maximized. On the other hand, minimizing PC_2 both the roughness and MRR responses will be maximized. Analogously, maximizing WPCA will maximize all responses, while minimizing it will minimize all responses.

To improve the end milling process, the roughness responses must be minimized, while material removal rate must be maximized. Thus, the study of the eigenvectors shows that it is impossible to minimize the roughness responses and maximize MRR simultaneously.

In this case, to comply with the objectives of the second part of this paper, two strategies will be proposed and compared: (a) to maximize WPCA and (b) to minimize WPCA. Probably, these multivariate optimization approaches by the WPCA method can lead to MRR minimization, or roughness surface maximization.

In both cases, using the GRG algorithm to solve the system of Eq. (3), the maximization and minimization of WPCA can be established according to Eqs. (15) and (16), respectively. The constraint of the experimental region $\mathbf{x^T x} \leq 2^2$ was considered, since ρ for CCD with control factors $k = 4$ is 2. Table 9 exhibits the optimal solution found.

$$\text{Maximize } WPCA = \lambda_1(PC_1) + \lambda_2(PC_2)$$
$$s.t : g(x) = x^T x \leq 2^2$$
(15)

and,

$$\text{Minimize } WPCA = \lambda_1(PC_1) + \lambda_2(PC_2)$$
$$s.t : g(x) = x^T x \leq 2^2.$$
(16)

In Table 9, Target and Nadir values of each original response were determined by individual constraint minimization (for roughness responses) and individual

1676

J Braz. Soc. Mech. Sci. Eng. (2017) 39:1663–1681

Table 9 Optimal solutions for the dry end milling process obtained with WPCA method

Optimal solution	Parameters				Quality					Productivity
	f_z	a_p	V_c	a_e	R_a	R_y	R_z	R_q	R_t	MRR
Targets (ζ_{y_j})	0.15	1.13	325	16.5	0.47	2.71	2.32	0.55	2.72	77.38
Nadir value	–	–	–	–	1.62	8.47	7.48	1.96	8.60	10.91
Mean values	–	–	–	–	1.49	6.92	6.37	1.74	7.07	34.57
Max WPCA	0.24	1.02	346	16.58	2.00	9.54	8.91	2.40	9.69	53.71
Min WPCA	0.05	1.07	327	16.39	0.47	2.73	2.32	0.55	2.75	11.01
Units	mm/tooth	mm	m/min	mm	μm	μm	μm	μm	μm	cm³/min

constraint maximization (for MRR response), such as $\zeta_{y_i} = \underset{x \in \Omega}{\text{Min}} \left[\hat{y}_j(x)\right]$ and $\zeta_{y_i} = \underset{x \in \Omega}{\text{Max}} \left[\hat{y}_j(x)\right]$, respectively. The target value corresponds to the best possible values, while Nadir value corresponds to the worst values. These values are considered as specification limits for the optimization problem.

As expected, the achieved optimum solutions by the WPCA method do not satisfy the end milling process improvement. It can be observed that when WPCA is maximized, the method tends to the MRR optimal values, while, at the same time, obtains high roughness values which are outside the specifications limits. On the other hand, when WPCA is minimized, the WPCA method tends to the roughness optimal values, in detriment of productivity.

4.4 Optimization by the weighted principal component analysis combined with Taguchi's signal-to-noise ratio method (SNR-WPCA)

Although the WPCA method can be very useful to eliminating correlated responses that will be optimized, they may conduct the results to inadequate optimum solutions if there are variables in the set with inverse directions of optimization. The results previously reported by the WPCA method showed that the maximization or minimization of the principal components favored some end milling characteristics and not others. Therefore, the WPCA method was applied to a new optimization to improve these results through standardization of optimization objectives of the original responses. For this, the Taguchi's signal-to-noise ratio (SNR) was applied before principal components analysis. In this part of the experiment, the steps previously described were developed.

4.4.1 Step A. Taguchi's signal-to-noise ratio and RSM models

The Taguchi's signal-to-noise ratio was calculated according to Eq. (4) for average surface roughness (R_a), maximum surface roughness (R_y), root-mean-square roughness (R_q), ten-point height (R_z), maximum peak to valley (R_t), and

according to Eq. (5) for material removal rate (MRR). The calculated values for SNR/R_a, SNR/R_y SNR/R_z SNR/R_q SNR/R_t, and SNR/MRR are presented in Table 8. Then, the OLS algorithm was applied on normalized responses, and the results can be observed in Table 10. It can be noted that all expressions presented lower error S values and the regression p-value were less than 5 % of significance. The Adj.R^2 value is above 85 %. All the residuals are normal. Thus, the ANOVA results show that the final full quadratic models are reliable and can be used for the optimization of this process.

4.4.2 Step B. Principal component analysis for the Taguchi's SNR responses and RSM models

Once the original responses were normalized by Taguchi's signal-to-noise ratio, PCA was performed on the data, considering the correlation matrix. The principal components scores were extracted and stored (Table 8) with their respective eigenvalues and eigenvectors (Table 11). PC_1 and PC_2 are responsible for the explanation of 99.1 % of the variation structure within the six SNR responses (Table 11). The multivariate outlier's detection (squared Mahalanobis distances) showed no unusual points (Fig. 5). Furthermore, it can be noted that PC_1 is mostly related to standardized roughness and that PC_2 relate to SNR-MRR (Table 11). These analyses imply that both PC_1 and PC_2 are necessary to form the SNR-WPCA index.

The OLS algorithm applied on PC_1 and PC_2 yielded the results that can be observed in Table 10. The ANOVA results show that the final full quadratic models are reliable and can be used for the optimization of this process.

4.4.3 Step C. SNR-WPCA index and RSM models

Finally, the SNR-WPCA multivariate objective function was developed considering the first and second principal component scores and their respective eigenvalues, ($\lambda_1 = 5.178$) and ($\lambda_2 = 0.762$) as weights, yielding the following:

$$\text{SNR-WPCA} = \lambda_1(\text{SNPC}_1) + \lambda_2(\text{SNPC}_2). \tag{18}$$

Table 10 Estimated coefficients for the final quadratic models and ANOVA results

Coefficient	Signal-to-noise ratio responses						Principal component		SNR-WPCA
	SNR/R_a	SNR/R_y	SNR/R_z	SNR/R_q	SNR/R_t	SNR/MRR	SNR/PC$_1$	SNR/PC$_2$	
Constant	**−4.147**	**−17.121**	**−16.512**	**−5.429**	**−17.296**	**30.772**	**−0.482**	**−0.038**	**−2.522**
f_z	**−1.891**	**−2.245**	**−2.129**	**−2.050**	**−2.221**	**3.171**	**−2.790**	**0.116**	**−10.191**
a_p	**0.413**	0.167	**0.256**	**0.360**	0.165	**3.171**	0.144	**0.889**	**2.209**
V_c	−0.136	0.025	0.010	−0.084	0.020	**0.670**	−0.085	**0.145**	0.456
a_e	−0.043	−0.035	−0.066	−0.056	−0.071	**0.794**	−0.115	**0.174**	−1.249
f_z^2	**0.590**	**0.532**	**0.442**	**0.549**	**0.538**	**−0.595**	**0.682**	0.071	**−0.834**
a_p^2	**0.384**	**0.212**	**0.314**	**0.361**	**0.226**	**−0.595**	**0.412**	−0.049	**2.744**
V_c^2	0.022	−0.047	−0.022	0.008	−0.060	0.016	−0.022	−0.006	0.529
a_e^2	0.021	0.026	−0.001	0.014	−0.015	0.005	0.013	−0.005	0.713
$f_z \times a_p$	**0.282**	0.126	0.196	**0.266**	0.138	0.000	0.253	0.070	0.181
$f_z \times V_c$	−0.176	−0.052	−0.100	−0.141	−0.069	−0.000	−0.133	−0.050	−1.909
$f_z \times a_e$	0.013	0.053	0.097	−0.003	0.114	0.000	0.065	0.016	1.531
$a_p \times V_c$	0.116	0.013	0.044	0.118	−0.039	−0.000	0.066	0.021	−0.824
$a_p \times a_e$	**−0.287**	**−0.261**	−0.198	**−0.253**	**−0.270**	0.000	**−0.316**	−0.075	**−0.511**
$V_c \times a_e$	−0.061	−0.134	−0.089	−0.081	−0.136	−0.000	−0.125	−0.019	0.523
Adj.R^2 (%)	92.76	93.99	93. 89	94.79	93.54	98.96	95.18	96.49	87.87
Standard error (S)	0.443	0.445	0.440	0.392	0.460	0.435	0.499	0.163	2.689
Regression p value	0.000	0.000	0.000	0.000	0.000	0.000	0.000	0.000	0.000
VIF	<1.10	<1.10	<1.10	<1.10	<1.10	<1.10	<1.50	<1.50	<1.50
Normality (AD) test	0.274	0.237	0.210	0.235	0.154	1.257	0.297	0.547	0.485
Normality (AD) p value	0.635	0.762	0. 844	0.769	0.951	<0.005	0.565	0.146	0.215
Curvature p value	0.000	0.000	0.000	0.000	0.000	*	0.001	0.144	0.001

Bold values represent the individually significant terms (p value <5 %)

Table 11 Principal component analysis: SNR-WPCA method

Eigenvalue (λ_{ij})	5.178	0.762	0.050	0.007	0.002	0.000
Proportion	0.863	0.127	0.008	0.001	0.000	0.000
Cumulative	0.863	0.990	0.998	1.000	1.000	1.000
Eigenvectors (e_{ij})	SNR-PC$_1$	SNR-PC$_2$	SNR-PC$_3$	SNR-PC$_4$	SNR-PC$_5$	SNR-PC$_6$
SNR-R_a	0.427	0.217	0.638	−0.299	−0.364	0.377
SNR-R_y	0.437	0.041	−0.453	−0.309	0.510	0.497
SNR-R_z	0.437	0.078	−0.222	0.797	−0.283	0.194
SNR-R_q	0.433	0.162	0.381	0.185	0.576	−0.524
SNR-R_t	0.437	0.036	−0.412	−0.381	−0.441	−0.547
SNR-MRR	−0.241	0.958	−0.156	−0.001	−0.003	−0.014

The SNR-WPCA values were stored in Table 8.

Considering the observations calculated in the SNR-PCA formulation, the values of the coefficients were estimated by the OLS algorithm, and the second-order mathematical model was developed as follows:

$$SNR\text{-}WPCA = -2.54 - 10.217f_z + 2.190a_p + 0.542v_c - 1.252a_e$$
$$- 0.837f_{z^2} + 2.751a_{p^2} + 0.527v_{c^2} + 0.714a_{e^2}$$
$$+ 0.185f_z \times a_p - 1.908f_z \times v_c + 1.528f_z \times a_e$$
$$- 0.820a_p \times v_c - 0.516a_p \times a_e + 0.520v_c \times a_e .$$
$$(19)$$

Then, the ANOVA procedure was applied to check for adequacies of the model as well as their adjustment. Table 10 presents the obtained coefficients for the final full quadratic model and the main results of the ANOVA. Since the regression p value presented less than 5 % of significance and lower error S value was presented, it can be seen that the expression SNR-WPCA is adequate. Regarding adjustments, the model presented Adj.R^2 values above 85 %, indicating a good adjustment. Furthermore, the calculated curvature p values show that the experimental space
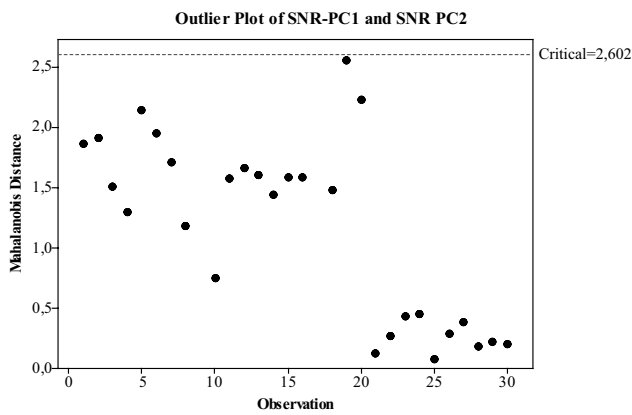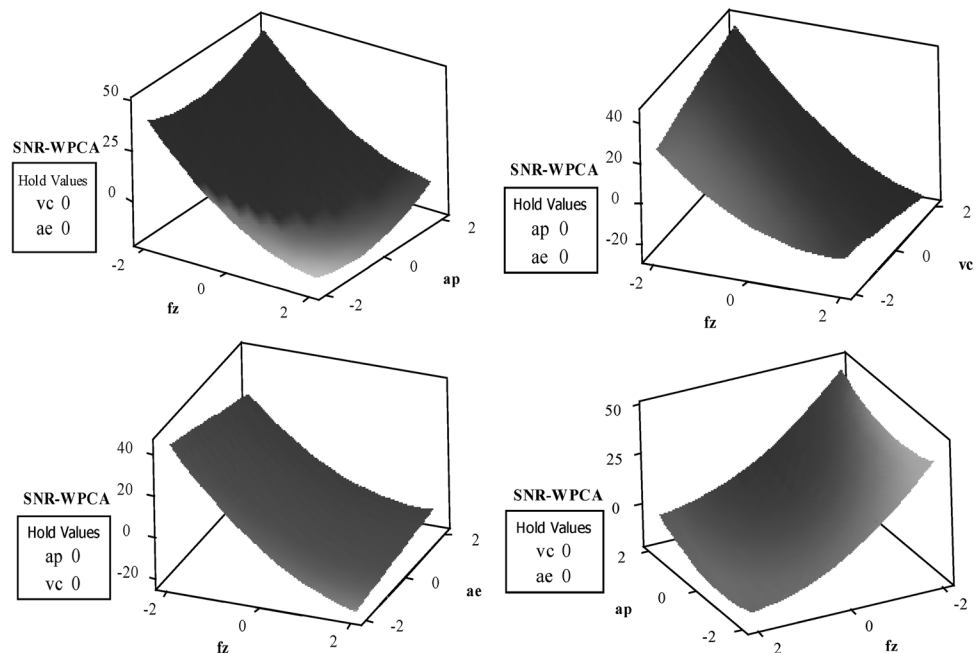
Fig. 5 Multivariate outlier's detection for SNR-WPCA method

for the SNR-WPCA multivariate objective response falls within the curvature region. The result of the normality test for the residuals demonstrates that the residuals are normal and uncorrelated for SNR-WPCA model (p value >5 % of significance). Even though some non-significant terms were found, their exclusion from the complete model increased the error S and reduced Adj.R^2. A full second-order model was then considered to surpass this problem. Therefore, the ANOVA results showed that the developed model is reliable and can be used in optimizing the dry end milling process.

Figure 6 represents the SNR-WPCA multivariate objective function as a function of the parameters feed per tooth (f_z), axial depth of cut (a_p), cutting speed (V_c), and radial depth of cut (a_e).

4.4.4 Step D. SNR-WPCA index and RSM models

Employing the GRG algorithm available from Microsoft Excel's Solver® routine for the system of Eq. (8), the maximization of the set of pre-processed response can be established according to Eq. (20). The non-linear constraint $\mathbf{x^T x} \leq 2^2$ was also considered.

$$\text{Maximize SNR-WPCA} = \lambda_1(\text{SNRPC}_1) + \lambda_2(\text{SNRPC}_2)$$
$$s.t : g(\mathbf{x}) = \mathbf{x^T x} \leq 2^2. \tag{20}$$

The maximization of the SNR-WPCA was used due to the mathematical nature of the signal-to-noise ratio; it must be always maximized. In this case, it is not a problem. Examining the eigenvectors (Table 11), it is possible to observe that the direction of optimization (or direction of correlation) between the PC1 and all the roughness responses is positive, while the direction of optimization (or direction of correlation) between the PC1 and MRR is negative. On the other hand, the direction of optimization between PC2 and all the responses is negative.

Since the first principal component consists mostly by the roughness and that the PC2 consists mostly by the MRR, it can be find out that when PC1 and PC2 are maximized, both roughness and MRR will be maximized. Therefore, all the objectives of the SNR responses will be achieved.

The optimization results are presented in Table 12 and can be compared with the Targets (ζ_{yi}) and Nadir values of the original responses.

Fig. 6 SNR-WPCA surface plot as a function of the end milling parameters

Table 12 Optimal solutions for the dry end milling process obtained with the SNR-WPCA method

Optimal solution	Parameters				Quality					Productivity
	f_z	a_p	V_c	a_e	R_a	R_y	R_z	R_q	R_t	MRR
Targets (ζ_{y_j})	0.15	1.13	325	16.5	0.47	2.71	2.32	0.55	2.72	77.38
Nadir value	–	–	–	–	1.62	8.47	7.48	1.96	8.60	10.91
Mean values	–	–	–	–	1.49	6.92	6.37	1.74	7.07	34.57
Max WPCA-SNR	0.08	1.62	331	15.49	0.82	3.84	3.56	0.96	3.89	26.59
Units	mm/tooth	mm	m/min	mm	μm	μm	μm	μm	μm	cm^3/min

According to the results present in Table 12, it can be observed that to maximize the MRR, while minimizing surface quality simultaneously, $f_z = 0.08$ mm/tooth, $a_p = 1.62$ mm, $V_c = 331$ m/min, and $a_e = 15.49$ mm are the values that attained the desired quality conditions using the SNR-WPCA method for dry end milling process.

Similar results were also obtained by Costa et al. [1]. The authors analysed the optimal parameters in a multi-objective optimization problem, in end milling process, to find at the same time, the maximum volume of removed material, and minimum surface roughness. In this article, $f_z = 0.09$ mm/tooth, $a_p = 1.73$ mm, $V_c = 333.78$ m/min, and $a_e = 16.20$ mm have been considered as the optimal cutting parameters to obtain values of 0.91, 4.34, 3.95, 1.06, and 4.44 μm (R_a, R_y, R_z, R_q, R_t, respectively), while a value of 33.88 cm^3/min has been obtained for MRR.

There are some physical explanations of the AISI 1045 end milling process that can justify the results found from this study. For example, the lower feed per tooth (f_z) minimizes the roughness of the part, because it promotes a geometric effect of the inserts on the tips of peaks of the milled surface texture irregularities. The depth of cut (a_p) obtained, near the level (+1) of DOE design, allows the mill to work with the main cutting edge and not just the nose radius ($r = 0.8$ mm). This makes it easier to shear the workpiece material and prevents the formation of a lateral flow on the chip, which could harm the finish and increase the roughness [40]. The larger the depth of cut the greater the productivity. The radial depth of cut (a_e) obtained, near the level (−1) of DOE design, enables the mill to work with its centre within the workpiece, with a ratio a_e/Dc of around 62 %. This ratio of radial depth of cut with cutting diameter (Dc) is considered optimal in terms of tool-workpiece engagement for asymmetrical down cut end mill, which causes it less prone to the vibration process [40]. The smaller the vibration the lower the surface roughness. The cutting speed (V_c) obtained per optimization method, near to level (0) of DOE design, enables the mill to work on a medium rotation. This makes it less likely that a vibration is brought to the rotation system of the machine tool and workpiece, since the machine used in the tests has longer than 10 years.

Thangarasu, Devaraj, and Sivasubramanian [32], Chahal et al. [33] and Singh et al. [35] have put forward the same

Table 13 Optimal solutions for the dry end milling process obtained with the SNR-WPCA method

Experiments	R_a	R_y	R_z	R_q	R_t
1	0.89	3.92	3.49	1.01	3.99
2	0.87	4.49	3.95	1.04	4.26
3	0.85	4.31	3,87	1.01	4.24

arguments, as the ones referred to above when roughness and MRR have been analysed in the end milling process. Ginta et al. [31] have also affirmed that an increase in cutting speed, axial depth of cut, and feed per tooth leads to increase in the surface roughness.

Furthermore, all optimized responses were established within the specification limits and relatively close to their Utopia point, which suggests that this approach gives a better solution than the WPCA method.

The numerical results indicate that the solutions found by WPCA-SNR approach were characterized as more appropriate optimal point in relation to one obtained with the WPCA method. Thus, the SNR-WPCA method showed itself to be a good technique to the optimization of the AISI 1045 dry end milling process.

5 Confirmation experiments

To verify the reproducibility of the results, a series of three confirmation experiments were run with the optimal combination of the dry end milling parameters, i.e., $f_z = 0.08$ mm/tooth, $a_p = 1.62$ mm, $V_c = 331$ m/min, and $a_e = 15.49$ mm. Table 13 presents these results and shows that most of the responses presented real values close to the predicted ones. It can be observed here that the SNR-WPCA method successfully conducted the process to a compatible result with the expected objectives.

6 Conclusion

This paper presents an approach, called weighted principal component analysis, combined with Taguchi's

signal-to-noise ratio (SNR-WPCA). SNR-WPCA was developed to optimize multiple correlated responses presenting different objectives optimization. Although capable of considering the correlation between the responses, the weighted principal component analysis (WPCA) can conduct the results to inadequate optimum solutions when the multiple responses present conflicting objectives of optimization. We proposed here a standardization of the optimization objectives of the original responses, by Taguchi's signal-to-noise, before principal component analysis. Response Surface Methodology, applied to model the dry end milling characteristics, developed statistically significant mathematical models.

The numerical results indicate that the solution found by SNR-WPCA approach was characterized as a more appropriate optimal point in relation to one obtained with the WPCA. Considering the SNR-WPCA method, $f_z = 0.08$ mm/tooth, $a_p = 1.62$ mm, $V_c = 331$ m/min, and $a_e = 15.49$ mm are the optimal parameters for minimize roughness, and maximize material removal rate, simultaneously.

On the other hand, the results reported by the WPCA method showed that the maximization or minimization of this function favors some characteristics and not others. I.e., when WPCA is maximized, the optimized MRR is established within the specification limits and relatively close to his target. However, this approach presents high roughness values. The opposite is also true. When WPCA is minimized, the optimized roughness responses are established very close to their targets and within the specification limits.

Therefore, the SNR-WPCA method showed itself capable to surpass the drawbacks of the WPCA method. The SNR-WPCA method showed itself to be a good technique to the optimization of the AISI 1045 dry end milling process when the multiple quality characteristics measured are highly correlated and with different optimization objectives.

The models' capability of predicting the results was verified by the confirmation experiments; low errors were observed between the theoretical and the real values.

Finally, the results are particularly useful for scientists and engineers to determine which parameters of the end milling process without cutting fluids are able to achieve, at the same time, the maximum rate of removed material, and minimum surface roughness.

References

1. Costa DMD, Brito TG, De Paiva AP et al (2016) A normal boundary intersection with multivariate mean square error approach for dry end milling process optimization of the AISI 1045 steel. J Clean Prod. doi:10.1016/j.jclepro.2016.01.062

2. Paiva AP, Costa SC, Paiva EJ et al (2010) Multi-objective optimization of pulsed gas metal arc welding process based on weighted principal component scores. Int J Adv Manuf Technol 50:113–125. doi:10.1007/s00170-009-2504-y

3. Moshat S, Datta S, Bandyopadhyay A, Pal PK (2010) Parametric optimization of CNC end milling using entropy measurement technique combined with grey-Taguchi method. Int J Eng Sci Technol 2:1–12. doi:10.4314/ijest.v2i2.59130

4. Montgomery DC (2012) Design and analysis of experiments. 8th edn. Wiley, Incorporated. ISBN 1118214714, 9781118214718

5. Bratchell N (1989) Multivariate response surface modelling by principal components analysis. J Chemom 3:579–588. doi:10.1002/cem.1180030406

6. Paiva AP, Ferreira JR, Balestrassi PP (2007) A multivariate hybrid approach applied to AISI 52100 hardened steel turning optimization. J Mater Process Technol 189:26–35. doi:10.1016/j.jmatprotec.2006.12.047

7. Costa DMD, Paula TI, Silva PAP, Paiva AP (2016) Normal boundary intersection method based on principal components and Taguchi' s signal-to-noise ratio applied to the multiobjective optimization of 12L14 free machining steel turning process. doi:10.1007/s00170-016-8478-7

8. Lopes LGD, Brito TG, De Paiva AP et al (2016) Computers & industrial engineering robust parameter optimization based on multivariate normal boundary intersection. Comput Ind Eng 93:55–66. doi:10.1016/j.cie.2015.12.023

9. Lu HS, Chang CK, Hwang NC, Chung CT (2009) Grey relational analysis coupled with principal component analysis for optimization design of the cutting parameters in high-speed end milling. J Mater Process Technol 209:3808–3817. doi:10.1016/j.jmatprotec.2008.08.030

10. Su CT, Tong LI (1997) Multi-response robust design by principal component analysis. Total Qual Manag 8:409–416. doi:10.1080/0954412979415

11. Antony J (2000) Multi-response optimization in industrial experiments using Taguchi's quality loss function and principal component analysis. Qual Reliab Eng Int 16:3–8. doi:10.1002/(SICI)1099-1638(200001/02)

12. Prabhu S, Vinayagam BK (2014) Multiobjective optimization of ELID grinding process using grey relational analysis coupled with principal component analysis. Adv Mech Eng 6:1–12. doi:10.1155/2014/878510

13. Fung CP, Kang PC (2005) Multi-response optimization in friction properties of PBT composites using Taguchi method and principle component analysis. J Mater Process Technol 170:602–610. doi:10.1016/j.jmatprotec.2005.06.040

14. Tong LI, Wang CH, Chen HC (2005) Optimization of multiple responses using principal component analysis and technique for order preference by similarity to ideal solution. Int J Adv Manuf Technol 27:407–414. doi:10.1007/s00170-004-2157-9

15. Dubey AK, Yadava V (2008) Multi-objective optimization of Nd: YAG laser cutting of nickel-based superalloy sheet using orthogonal array with principal component analysis. Opt Lasers Eng 46:124–132. doi:10.1016/j.optlaseng.2007.08.011

16. Murthy KS, Rajendran I (2012) Optimization of end milling parameters under minimum quantity lubrication using principal component analysis and grey relational analysis. J Braz Soc Mech Sci Eng 34:253–261. doi:10.1590/S1678-58782012000300005

17. Rocha LCS, Paiva AP, Paiva EJ, Balestrassi PP (2015) Comparing DEA and principal component analysis in the multiobjective optimization of P-GMAW process. J Braz Soc Mech Sci Eng. doi:10.1007/s40430-015-0355-z

18. Salmasnia A, Kazemzadeh RB, Taghi S, Niaki A (2012) An approach to optimize correlated multiple responses using principal component analysis and desirability function. 835–846. doi:10.1007/s00170-011-3824-2

19. Ribeiro JS, Teófilo RF, Augusto F, Ferreira MMC (2010) Simultaneous optimization of the microextraction of coffee volatiles using response surface methodology and principal component analysis. Chemom Intell Lab Syst 102:45–52. doi:10.1016/j.chemolab.2010.03.005

20. Lopes LGD, Gomes JHDF, De Paiva AP et al (2013) A multivariate surface roughness modeling and optimization under conditions of uncertainty. Meas J Int Meas Confed 46:2555–2568. doi:10.1016/j.measurement.2013.04.031

21. Delchambre L (2014) Weighted principal component analysis: a weighted covariance eigendecomposition approach. Mon Not R Astron Soc 446:3545–3555. doi:10.1093/mnras/stu2219

22. Das MK, Kumar K, Barman TK, Sahoo P (2014) Application of artificial bee colony algorithm for optimization of MRR and surface roughness in EDM of EN31 tool steel. Procedia Mater Sci 6:741–751. doi:10.1016/j.mspro.2014.07.090

23. Pinto da Costa JF, Alonso H, Roque L (2011) A weighted principal component analysis and its application to gene expression data. IEEE/ACM Trans Comput Biol Bioinform 8:246–252. doi:10.1109/TCBB.2009.61

24. Peruchi RS, Balestrassi PP, De Paiva AP et al (2013) A new multivariate gage R&R method for correlated characteristics. Int J Prod Econ 144:301–315. doi:10.1016/j.ijpe.2013.02.018

25. Wu FC, Chyu CC (2004) Optimization of correlated multiple quality characteristics robust design using principal component analysis. J Manuf Syst 23:134–143. doi:10.1016/S0278-6125(05)00005-1

26. Fu T, Zhao J, Liu W (2012) Multi-objective optimization of cutting parameters in high-speed milling based on grey relational analysis coupled with principal component analysis. Front Mech Eng 7:445–452. doi:10.1007/s11465-012-0338-z

27. Liao HC (2006) Multi-response optimization using weighted principal component. Int J Adv Manuf Technol 27:720–725. doi:10.1007/s00170-004-2248-7

28. Bertolini AC, Schiozer DJ (2016) Principal component analysis for reservoir uncertainty reduction. J Braz Soc Mech Sci Eng 38:1345–1355. doi:10.1007/s40430-015-0377-6

29. Wu FC, Chyu CC (2004) Optimization of correlated multiple quality characteristics robust design using principal component analysis. J Manuf Syst 2:134–143. doi:10.1016/S0278-6125(05)00005-1

30. Zhang M, Anwer N, Stockinger A et al (2013) Discrete shape modeling for skin model representation. Proc Inst Mech Eng Part B J Eng Manuf 227:672–680. doi:10.1177/0954405412466987

31. Turnad LG, Amin AKMN, Karim ANM, et al (2008) Modeling and optimization of tool life and surface roughness for end milling titanium alloy Ti–6Al–4V using Uncoated WC-Co inserts. In: Curtin University of Technology Science and Engineering International Conference 2008, 24–27 November 2008

32. Thangarasu VS, Devaraj G, Sivasubramanian R (2012) High speed CNC machining of AISI 304 stainless steel; Optimization of process parameters by MOGA. Int J Eng Sci Technol 4:66–77

33. Chahal M, Singh V, Garg R, Kumar S (2013) To estimate the range of process parameters for optimization of surface roughness & material removal rate in CNC milling 4:4556–4563

34. Brito TG, Paiva AP, Ferreira JR et al (2014) A normal boundary intersection approach to multiresponse robust optimization of the surface roughness in end milling process with combined arrays. Precis Eng 38:628–638. doi:10.1016/j.precisioneng.2014.02.013

35. Singh C, Bhogal SS, Pabla Dr BS et al (2014) Empirical modeling of surface roughness and metal removal rate in CNC milling operation. Int J Innov Technol Res 2:1120–1126

36. Kumar G, Davis R (2014) A comparative analysis of surface roughness and material removal rate in milling operation of AISI 410 steel and aluminium 6061. Int J Eng Res Appl 4:89–93

37. Bhogal SS, Sindhu C, Dhami SS, Pabla BS (2015) Minimization of surface roughness and tool vibration in CNC milling operation. J Optim 2015:1–13. doi:10.1155/2015/192030

38. Johnson RA, Wichern DW (2007) Applied multivariate statistical analysis, 6th edn. Pearson Educational, New Jersey. ISBN 9780131877153

39. Groot P, Postma G, Melssen W et al (2001) Application of principal component analysis to detect outliers and spectral deviations in near-field surface-enhanced Raman spectra. Anal Chim Acta 446:71–83. doi:10.1016/S0003-2670(01)01267-3

40. Trent EM, Wright PK (2000) Metal cutting, 4th edn. Butterworth Heinemann,USA